Eurasian Journal of Physics and Functional Materials

Volume 9 | Number 1

Article 3

Pages: 21 - 27

3-29-2025

Solubility of copper in ZrSe2

Postnikov M.S.
M.N. Miheev Institute of Metal Physics of Ural Branch of Russian Academy of Sciences, 620990, Ekaterinburg, Russia

Stashkova L.A.
M.N. Miheev Institute of Metal Physics of Ural Branch of Russian Academy of Sciences, 620990, Ekaterinburg, Russia

Shkvarin A.S.
M.N. Miheev Institute of Metal Physics of Ural Branch of Russian Academy of Sciences, 620990, Ekaterinburg, Russia, shkvarin@imp.uran.ru

Titov A.N.
M.N. Miheev Institute of Metal Physics of Ural Branch of Russian Academy of Sciences, 620990, Ekaterinburg, Russia

Recommended Citation

M.S., Postnikov; L.A., Stashkova; A.S., Shkvarin; and A.N., Titov (2025) "Solubility of copper in ZrSe2," *Eurasian Journal of Physics and Functional Materials*: Vol. 9: No. 1, Article 3.
DOI: https://doi.org/10.69912/2616-8537.1238

ORIGINAL STUDY

Solubility of Copper in $ZrSe_2$

Mikhail S. Postnikov, Lyudmila A. Stashkova, Alexey S. Shkvarin*, Alexander N. Titov

M.N. Miheev Institute of Metal Physics of Ural Branch of Russian Academy of Sciences, 620990, Ekaterinburg, Russia

Abstract

Previously obtained single crystals of Cu_xZrSe_2 show Cu contents up to x = 1. However, as a result of the solid phase reaction, the composition with maximum Cu content x = 0.45 is obtained. The process of copper dissolution in Cu_xZrSe_2 at x > 0.5 has been studied by DSC and X-ray diffraction methods to investigate the reasons preventing the composition x > 0.45 by solid phase reaction, as well as the possibility of avoiding these difficulties. It is concluded that the reason limiting the solubility of copper is the formation of a barrier layer on the surface of the copper particles.

1. Introduction

The layered transition metal dichalcogenides (LTMDs) and their intercalation compounds have been the subject of significant considerable interest over the past few decades. This is due to the notable physical properties that they possess [1—8] and the potential applications that they offer [9—13].

Recently synthesized $CuZrSe_2$ shows interesting properties [14]. In particular, a non-centrosymmetric crystal structure is expected for this material due to the unequal filling of van der Waals gaps by copper, which are tetrahedrally coordinated by selenium, see Fig. 1.

However, there is a surprising situation - conventional solid-phase synthesis can obtain a homogeneous material only in the range of copper content $0 < x \leq 0.5$. Further increase of the copper content leads to the precipitation of additional phases, preventing the use of this material for the study of properties. At the same time, when single crystals are grown by gas transport reactions, crystals with the composition Cu_1ZrSe_2 or close to it are quite stable. It is clear that only a small part of the initial polycrystalline sample is transformed into crystals. The crystals are therefore part of a multi-component and multiphase material. Nevertheless, the presence of such crystals means that the composition Cu_1ZrSe_2 is thermodynamically quite stable and the fact that we cannot obtain a homogeneous material with composition x > 0.5 means that the conditions under which the copper-rich compositions of the system are in a single-phase state are not fulfilled. The present work is devoted to the search for such conditions.

It should be noted that for intercalate compounds based on ZrS_2, isostructural $ZrSe_2$, the solubility of Fe, Co, Ni and Cu also does not exceed 50 mol% [15]. However, in these systems, single crystals cannot be synthesized for compositions above 50 mol% intercalant. At the same time, a spinel phase is formed in the Cu_xZrS_2 system at x = 0.5 [16]. Thus, the intercalation limit of ZrS_2 is not related to kinetic but to thermodynamic constraints. At the same time, known attempts of copper intercalation in $ZrSe_2$ were not only limited to low copper concentrations (x = 0.07), but were also performed in a material significantly contaminated with self-intercalated zirconium [17]. The Cu content range x = 0.5—1.0 in Cu_xZrSe_2 is under investigation for the first time in the present work.

2. Experiment

The polycrystalline sample of Cu_xZrSe_2 was synthesized using previously prepared $ZrSe_2$ and metallic copper. $ZrSe_2$ was obtained from the starting elements: Zr (99.95 %) and Se (99.99 %). The appropriate amount of the starting elements with a total sample mass of 3 g was sintered at 1000 °C for 7 days in sealed quartz ampoules with diameter 12 mm and length 120—130 mm, evacuated to 10^{-5} Torr in a tube furnace with a temperature gradient not exceeding 1 deg/cm. Then the ampoules were opened, the samples were ground in an agate mortar, pressed at a pressure

Received 21 November 2024; revised 1 February 2025; accepted 8 February 2025.
Available online 29 March 2025

* Corresponding author.
E-mail address: shkvarin@imp.uran.ru (A.S. Shkvarin).

https://doi.org/10.69912/2616-8537.1238

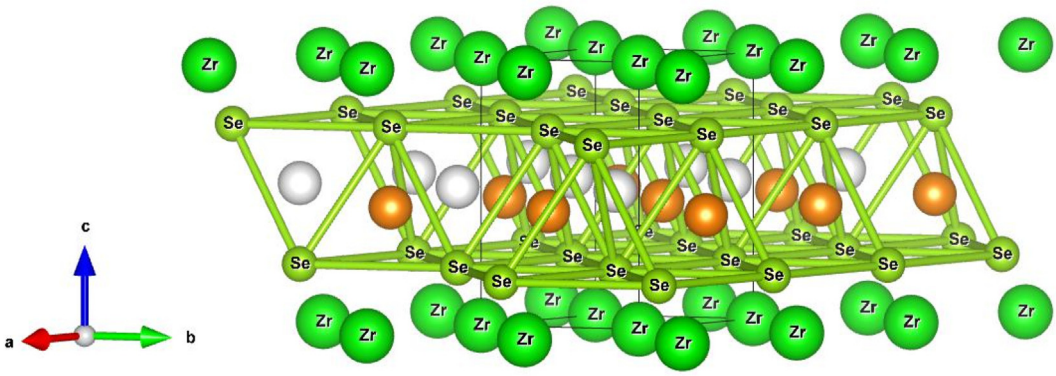

Fig. 1. Fragment of crystal structure for Cu_1ZrSe_2, orange sphere is filled by Cu tetra sites, white — empty one.

of 20 kg/mm^2, and annealed again under the same conditions for one week for homogenization. After this procedure, X-ray diffraction analysis did not show the presence of impurity phases.

The Cu_xZrSe_2 samples were prepared by the usual thermal intercalation procedure at room temperature [18]. Further annealing was performed in a muffle furnace at temperatures of 85 °C, 260 °C and 280 °C.

Calorimetric studies have been carried out with the using the equipment of the Collaborative Access Center «Testing Center of Nanotechnology and Advanced Materials» of the IMP UB RAS. Differential scanning calorimetry data were obtained using a STA 449 F3 Jupiter synchronous thermal analysis instrument (Netzsch) in a nitrogen atmosphere during heating and cooling in the temperature range 0—440 °C at a rate of 5 °C/min. The experimental data were processed using the NETZSCH Proteus Analysis® software package.

3. Result and discussion

Fig. 2 shows the diffractograms of Cu_xZrSe_2 samples in the Cu concentration range $0.5 \leq x \leq 1$ and for initial $ZrSe_2$ obtained at room temperature. The indexing

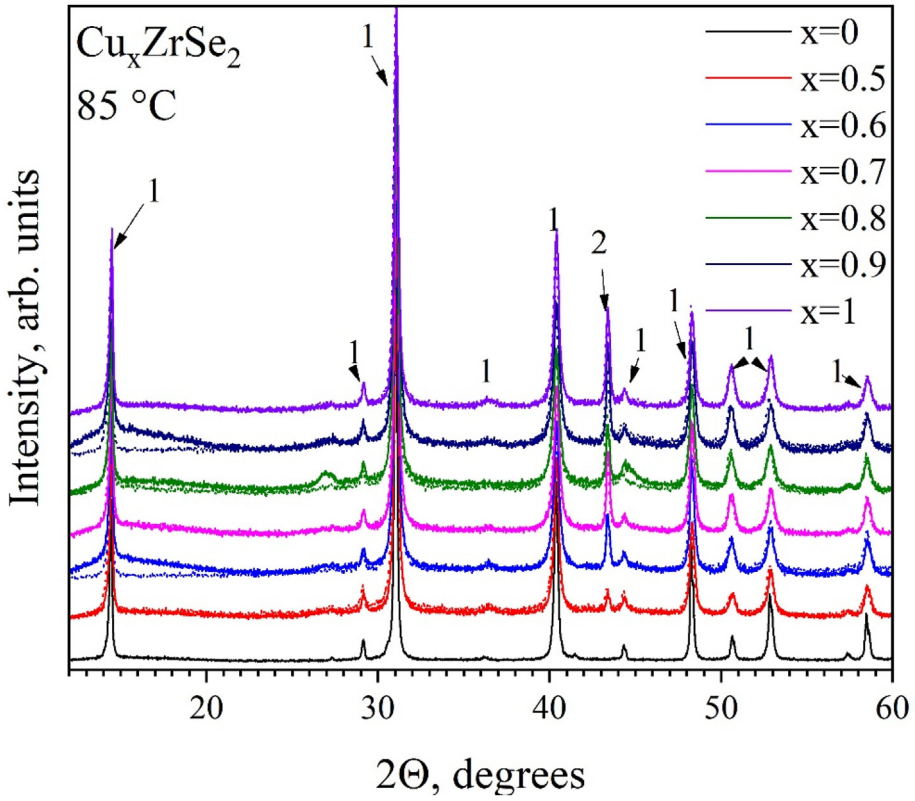

Fig. 2. Diffraction patterns for Cu_xZrSe_2 samples synthesized at room temperature. Arrows marked as 1 show main peaks of the layered Cu_xZrSe_2 phase. Arrow marked as 2 shows main peak of Cu phase.

showed that the structure of the main phase in all samples is described by the space group $P\bar{3}m1$. In addition, peaks other than the main phase were observed (labeled 2 in Fig. 1). Indexing showed that this peak belongs to the pure copper phase. As the relative intensity of this peak increases, it can be assumed that there is some limit to the solubility of copper in $ZrSe_2$ at room temperature.

No significant changes were observed after annealing at 85 °C for 72 h (see Figure S1 in the Supporting Data).

Since it is possible to obtain crystals with a higher Cu composition (up to $x = 1$) than polycrystalline samples [14] (where the solubility limit is about $x = 0.45$), it can be assumed that a higher temperature expands the solubility range. However, in this case it is not possible to simply increase the temperature (e.g., up to 500 °C) because parasitic phases are released [16]. Therefore, we used the differential scanning calorimetry (DSC) method to determine the temperatures of possible transitions. Fig. 3 shows DSC curves obtained by heating of Cu_xZrSe_2 samples ($x = 0.5$, 0.6, 0.7, 0.8, 0.9 and 1) in the temperature range 0–440 °C. The transition onset and end temperatures as well as the peak temperature were determined and are summarized in Table 1 and Figure S2 in the Supporting Data.

The peak in the temperature range of 150–260 °C is clearly visible. The thermal stability study of the Cu_1ZrSe_2 compound [19] showed that as the temperature increases, the copper dissolution process is accompanied by the copper selenide extraction process. Since only one peak is observed, only one process should be observed in this temperature range. A series of annealing's were performed at 260 and 280 °C for 48 h. The resulting diffractograms are shown in Fig. 4.

Table 1. The transition onset and end temperatures as well as the peak temperature for Cu_xZrSe_2.

Sample	T_{onset}	T_{peak}	T_{end}
$Cu_{0.5}ZrSe_2$	150	218	251
$Cu_{0.6}ZrSe_2$	153	200	236
$Cu_{0.7}ZrSe_2$	153	204	242
$Cu_{0.8}ZrSe_2$	149	192	239
$Cu_{0.9}ZrSe_2$	146	202	246
Cu_1ZrSe_2	129	219	264

It can be seen that the Cu peak disappears for the composition x = 0.5 and decreases for x = 0.6. No additional phases, such as copper selenides, are formed. The exothermic effect can only be related to the dissolution of copper in Cu_xZrSe_2. The degree of copper solubility in $ZrSe_2$ can be estimated from the ratio of the intensity of the main peak of copper to the intensity of the main peak of the layered phase (see Fig. 5).

It is easy to see that the solubility of copper increased for all compositions. The decrease in solubility with increasing copper concentration is most likely due to kinetic difficulties caused by a decrease in the number of possible positions.

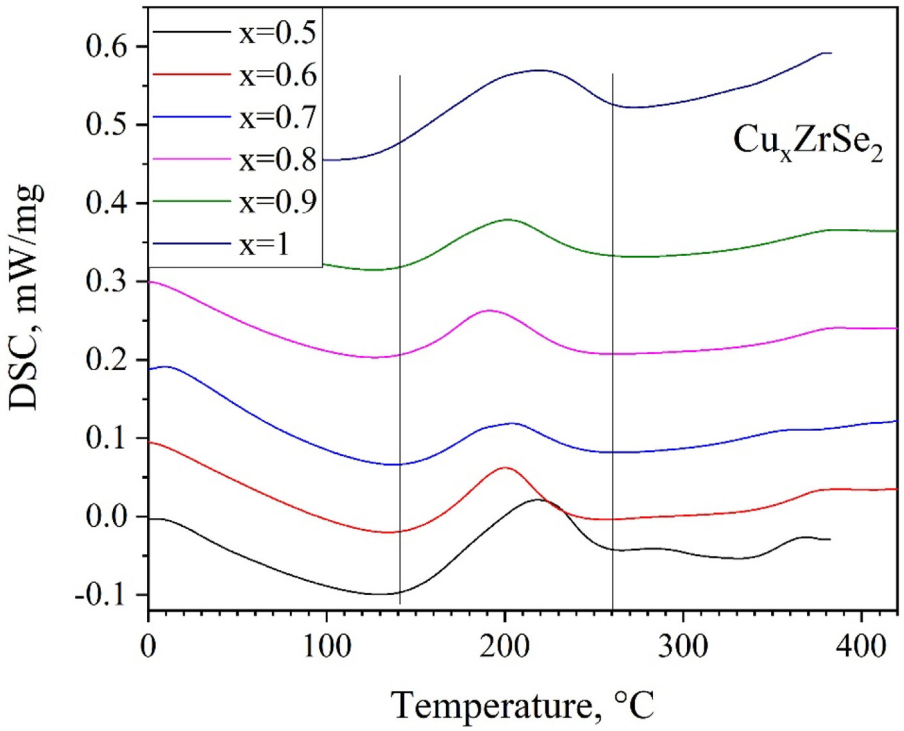

Fig. 3. DSC curves for Cu_xZrSe_2 samples.

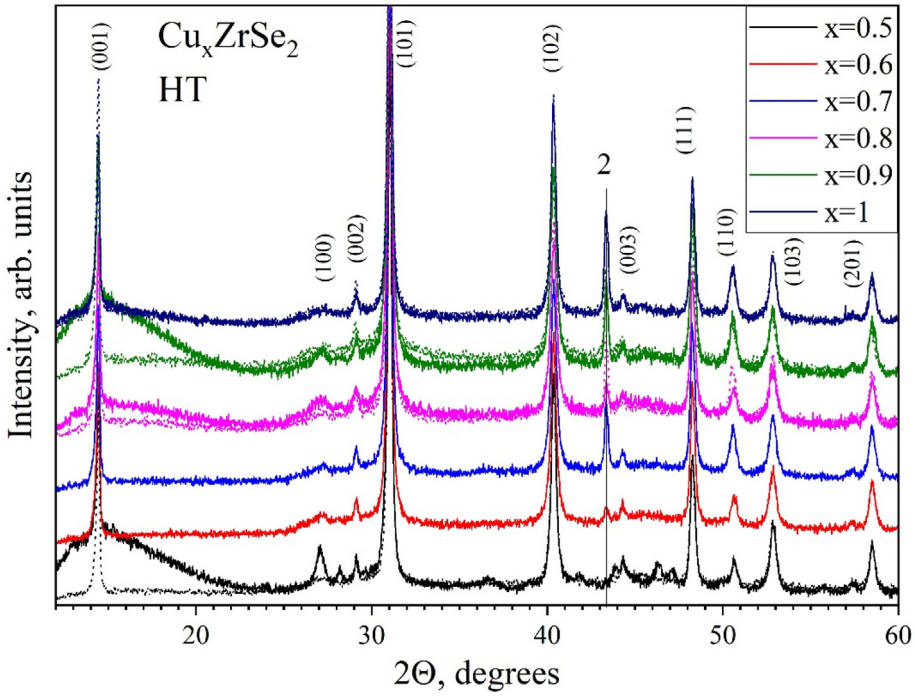

Fig. 4. Diffraction patterns of Cu_xZrSe_2 annealed at 260 (solid lines) and 280 (dot lines) °C. Arrow marked as 2 shows main peak of Cu phase.

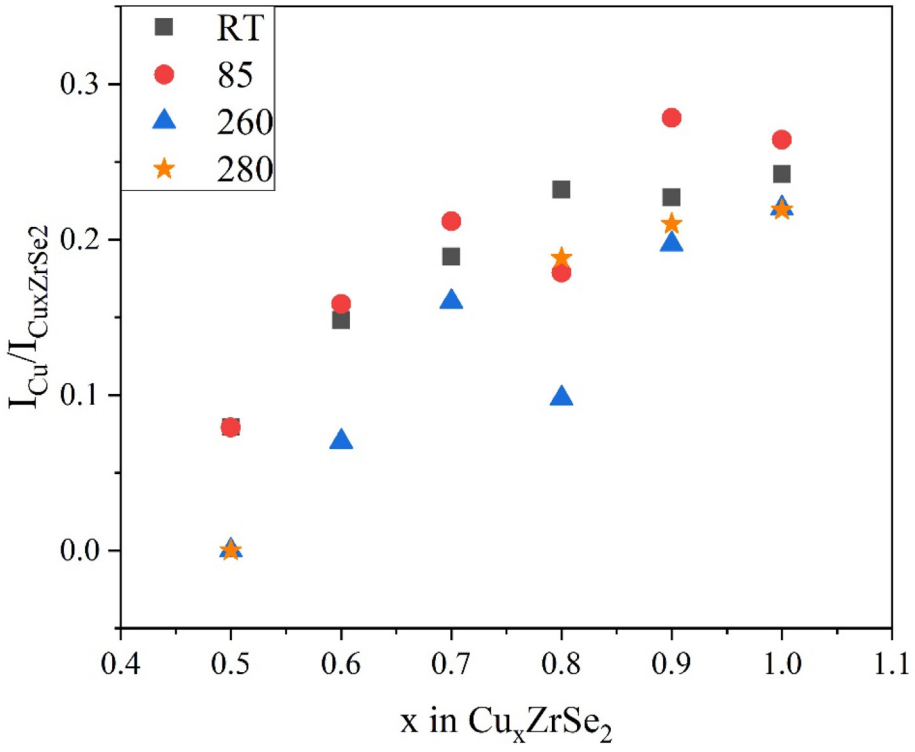

Fig. 5. Ratio of the intensity of the main peak of copper to the intensity of the main peak of the layered phase.

Repeated measurements of the DSC spectra (see Fig. 6) showed no peak in the temperature range 150–260 °C. The obvious explanation is the complete dissolution of all the copper capable of doing so. It is possible that the sample contains some more copper that is not in contact with the Cu_xZrSe_2 particles. This could be due to the presence of surface layers that prevent copper solubility. For example, the particles may be oxidized or covered with another layer of substance that interferes with the diffusion of copper

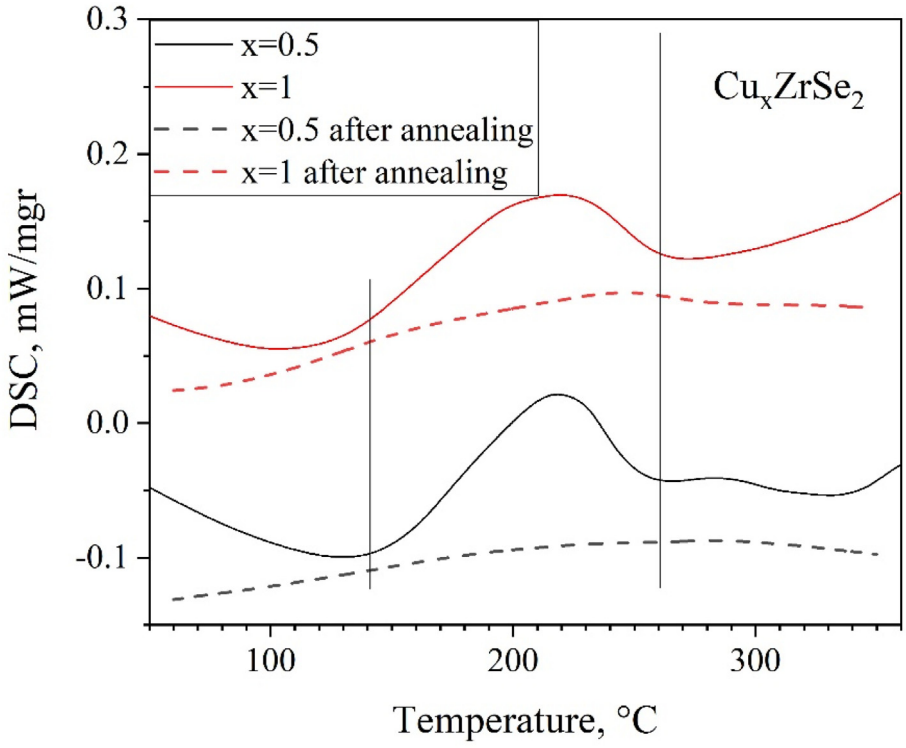

Fig. 6. DSC curves of Cu_xZrSe_2 samples for compositions $x = 1$ and $x = 0.5$ before and after annealing.

into the particles. Obviously, heating to temperatures above 350 °C can cause copper to be able to overcome this barrier. However, experience has shown that this is accompanied by the effects of parasitic phase formation. This explains the effect of the possibility of obtaining single crystals at high temperatures. Indeed, at such temperatures the barrier is probably not an obstacle to copper solubility. However, the growth of the crystals takes place in the presence of parasitic phase formation.

For the synthesis of homogeneous ceramic materials, it is therefore necessary to find methods of breaking the barrier that prevents the complete solubility of copper without heating. Our further work in this direction will be devoted to searching for such a method. Among such methods, mechanosynthesis, which consists of grinding and stirring the material after dissolution has ceased due to surface barriers, may be effective. However, the dispersibility of the material after mechanosynthesis may not allow the presence of copper to be observed due to the broadening of the diffraction lines. It is also possible that a significant increase in annealing time may also have an effect on the dissolution of undissolved copper.

4. Conclusions

The X-ray diffraction analysis shows the presence of metallic Cu in Cu_xZrSe_2 at $x > 0.5$, but the DSC does not show any reaction between Cu and Cu_xZrSe_2. The reason that limits the solubility of Cu in Cu_xZrSe_2 at $x > 0.5$ is the presence of surface difficulties at the Cu/Cu_xZrSe_2 interface. These difficulties probably arise in the process of copper dissolution, since they are not observed at copper concentrations $x < 0.5$. The reason for these difficulties may be the formation of an oxide layer on the surface of the copper particles during synthesis, and the source of oxygen may be oxygen adsorbed on the walls of the ampoule and the sample. For the successful synthesis of Cu_xZrSe_2 ceramic samples with copper content $x = 0.5–1.0$ it is necessary to find a way to prevent the formation of such a layer or a way to get rid of it without resorting to heating to temperatures above 350 °C.

Funding

Funding for this research was provided by: Russian Science Foundation (project No. 22-13-00361).

Conflicts of interest

There is no conflict of interest.

Acknowledgement

Funding for this research was provided by: Russian Science Foundation (project No. 22-13-00361).

Supporting data

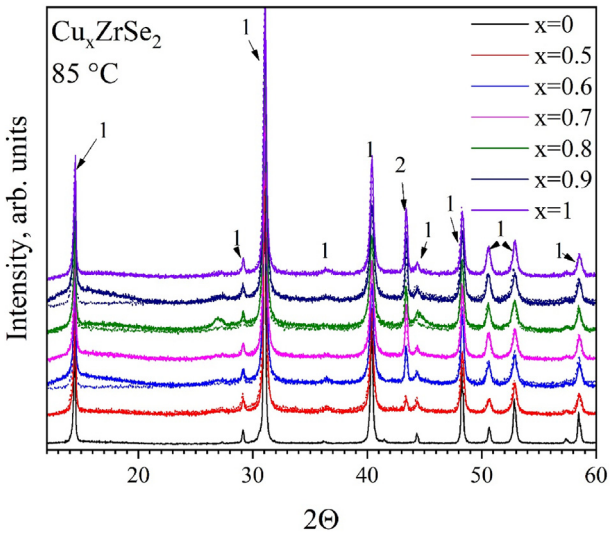

Fig. S1. Diffraction patterns for Cu_xZrSe_2 synthesized at 85° C. Arrows marked as 1 show main peaks of the layered Cu_xZrSe_2 phase. Arrow marked as 2 shows main peak of Cu phase. Diffraction patterns for Cu_xZrSe_2 synthesized at room temperature are shown as dots for comparison.

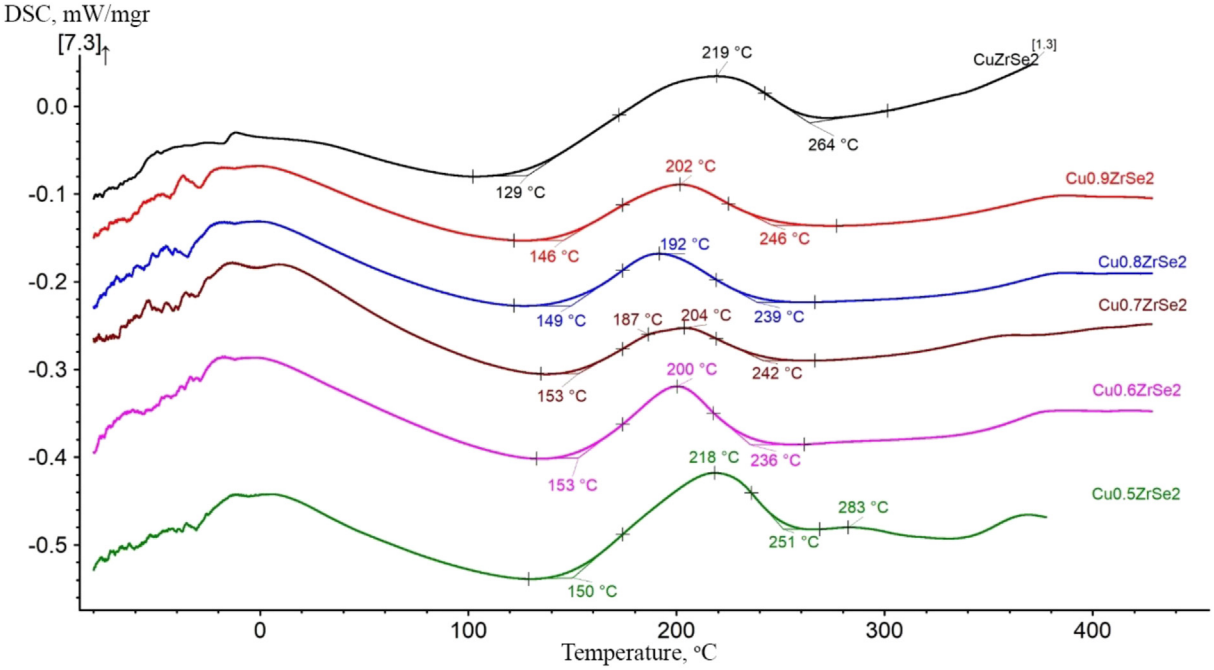

Fig. S2. DSC curves of Cu_xZrSe_2 samples.

References

[1] J.A. Wilson, A.D. Yoffe, The transition metal dichalcogenides discussion and interpretation of the observed optical, electrical and structural properties, Adv. Phys. 18 (1969) 193–335, https://doi.org/10.1080/00018736900101307.

[2] X. Zhao, T. Wang, C. Xia, X. Dai, S. Wei, L. Yang, Magnetic doping in two-dimensional transition-metal dichalcogenide zirconium diselenide, J. Alloys Compd. 698 (2017) 611–616, https://doi.org/10.1016/j.jallcom.2016.12.260.

[3] D.W. Bullett, Electronic band structure and bonding in transition metal layered dichalcogenides by atomic orbital methods, J. Phys. C Solid State Phys. 11 (1978) 4501–4514, https://doi.org/10.1088/0022-3719/11/22/007.

[4] Y.-T. Hsu, A. Vaezi, M.H. Fischer, E.-A. Kim, Topological superconductivity in monolayer transition metal dichalcogenides, Nat. Commun. 8 (2017) 14985, https://doi.org/10.1038/ncomms14985.

[5] E. Morosan, H.W. Zandbergen, B.S. Dennis, J.W.G. Bos, Y. Onose, T. Klimczuk, A.P. Ramirez, N.P. Ong, R.J. Cava, Superconductivity in Cu_xTiSe_2, Nat. Phys. 2 (2006) 544—550, https://doi.org/10.1038/nphys360.
[6] S. Manzeli, D. Ovchinnikov, D. Pasquier, O.V. Yazyev, A. Kis, 2D transition metal dichalcogenides, Nat. Rev. Mater. 2 (2017) 17033, https://doi.org/10.1038/natrevmats.2017.33.
[7] F. Yang, P. Hu, F.F. Yang, B. Chen, F. Yin, R. Sun, K. Hao, F. Zhu, K. Wang, Z. Yin, Emerging Enhancement and Regulation Strategies for Ferromagnetic 2D Transition Metal Dichalcogenides, Adv. Sci. 10 (2023), https://doi.org/10.1002/advs.202300952.
[8] V. Crépel, L. Fu, Anomalous Hall metal and fractional Chern insulator in twisted transition metal dichalcogenides, Phys. Rev. B 107 (2023) L201109, https://doi.org/10.1103/PhysRevB.107.L201109.
[9] R. Yang, Y. Fan, Y. Zhang, L. Mei, R. Zhu, J. Qin, J. Hu, Z. Chen, Y. Hau Ng, D. Voiry, S. Li, Q. Lu, Q. Wang, J.C. Yu, Z. Zeng, 2D Transition Metal Dichalcogenides for Photocatalysis, Angew. Chemie Int. Ed. 62 (2023), https://doi.org/10.1002/anie.202218016.
[10] Q.H. Wang, K. Kalantar-Zadeh, A. Kis, J.N. Coleman, M.S. Strano, Electronics and optoelectronics of two-dimensional transition metal dichalcogenides, Nat. Nanotechnol. 7 (2012) 699—712, https://doi.org/10.1038/nnano.2012.193.
[11] Y. Ominato, J. Fujimoto, M. Matsuo, Valley-Dependent Spin Transport in Monolayer Transition-Metal Dichalcogenides, Phys. Rev. Lett. 124 (2020) 166803, https://doi.org/10.1103/PhysRevLett.124.166803.
[12] S. Zhang, J. Li, X. Jin, G. Wu, Current advances of transition metal dichalcogenides in electromagnetic wave absorption: A brief review, Int. J. Miner. Metall. Mater. 30 (2023) 428—445, https://doi.org/10.1007/s12613-022-2546-9.
[13] M.J. Theibault, C. Chandler, I. Dabo, H.D. Abruña, Transition Metal Dichalcogenides as Effective Catalysts for High-Rate Lithium—Sulfur Batteries, ACS Catal. 13 (2023) 3684—3691, https://doi.org/10.1021/acscatal.3c00186.
[14] A.S. Shkvarin, A.I. Merentsov, M.S. Postnikov, E.G. Shkvarina, E.G. Dyachkov, E.V. Mostovshchikova, A.V. Koroleva, E.V. Zhizhin, A. N. Titov, Electronic structure of CuxZrSe2 with tetrahedrally-coordinated Cu atoms, Surf. Interfaces 55 (2024) 105334, https://doi.org/10.1016/j.surfin.2024.105334.
[15] F.W. Boswell, B.G. Yacobi, J.M. Corbett, Ordered phases in intercalation compounds of ZrS2 with Fe, Co, Ni and Cu, Mater. Res. Bull. 14 (1979) 1111—1118, https://doi.org/10.1016/0025-5408(79)90204-6.
[16] N. Matsumoto, T. Hagino, K. Taniguchi, S. Chikazawa, S. Nagata, Electrical and magnetic properties of $CuTi_2S_4$ and $CuZr_2S_4$, Phys. B Condens. Matter 284—288 (2000) 1978—1979, https://doi.org/10.1016/S0921-4526(99)02946-4.
[17] Z. Muhammad, K. Mu, H. Lv, C. Wu, Z. Rehman, M. Habib, Z. ur Rehman, M. Habib, Z. Sun, X. Wu, L. Song, Electron doping induced semiconductor to metal transitions in ZrSe 2 layers via copper atomic intercalation, Nano Res. 11 (2018) 4914—4922, https://doi.org/10.1007/s12274-018-2081-1.
[18] A.A. Titov, E.G. Shkvarina, A.I. Merentsov, A.A. Doroshek, A.S. Shkvarin, Y.M. Zhukov, A.G. Rybkin, S.V. Pryanichnikov, S.A. Uporov, A.N. Titov, Synthesis, structure and properties of the layered Cu x TiS 2 compounds, J. Alloys Compd. 750 (2018) 42—54, https://doi.org/10.1016/j.jallcom.2018.03.376.
[19] E.G. Shkvarina, A.S. Shkvarin, A.A. Titov, M.S. Postnikov, J.R. Plaisier, L. Gigli, M. Gaboardi, A.N. Titov, Thermal stability of the CuZrSe2, J. Solid State Chem. 328 (2023) 124307, https://doi.org/10.1016/j.jssc.2023.124307.